

# Effect of Thermomechanical Processing in the Intercritical Region on Hardenability of Austenite of a Dual-Phase Steel

M. Sarwar, E. Ahmad, and R. Priestner

(Submitted 19 January 2000; in revised form 9 July 2001)

Steels slabs containing different percentages of C, Mn, and Cr were intercritically heat treated and rolled at 780 and 790 °C; they were then quenched to produce dual-phase microstructure in order to study the martensitic hardenability of austenite present in them. It was found that rolling of the two-phase ( $\alpha + \gamma$ ) microstructure elongated austenite particles and also reduced the martensitic hardenability of austenite particles, probably because the rolling increased the  $\alpha/\gamma$  interfacial area, thus promoting the formation of ferrite during cooling. The martensite particles obtained in the rolled material were also elongated or “fibred” in the rolling direction. It was observed that the thermomechanical processing of a two-phase ( $\alpha + \gamma$ ) mixture has the detrimental effect of increasing the quenching power needed to yield a specific amount of martensite.

**Keywords** austenite, dual-phase steels, hardenability, martensite, thermomechanical working

## 1. Introduction

The characteristic microstructure of dual-phase steel consists of 20 to 25% Martensite Island in a soft and ductile matrix of ferrite. Dual-phase steels have unique mechanical properties, which include low proof strength and high tensile strength relative to conventional low-carbon formable steel. They also exhibit high work-hardening rates in the early stage of plastic deformation and good ductility during forming relative to their strength in the formed condition. The latter quality puts dual-phase steel high on the list of materials that are being considered by the automobile industry to reduce the weight of vehicles for improved economy. The conventional method for the production of dual-phase steels is annealing on carbon steel within the intercritical temperature range for a few minutes, followed by cooling at a rate fast enough to transform the austenite to martensite. The annealing temperatures control the amount of austenite present during intercritical annealing, which also controls the carbon content and the hardenability of the austenite.

Lawson and Matlock (1) expressed the constituents of steel after cooling from intercritical annealing temperature in the form of “Microstructure map”. Austenite→martensitic hardenability diagram derived by Priestner and Ajmal (2) from microstructure map in which percentage of the austenite is plotted versus cooling rate, which specifically the martensitic hardenability of austenite. This concept has also been used in the present study to describe the effect of thermomechanical process on hardenability of austenite.

M. Sarwar, PAEC, D.G. Khan, Pakistan; E. Ahmad, PAEC, PINSTECH, Nilore, Islamabad, Pakistan; and R. Priestner, Manchester Materials Science Center, Manchester, England. Contact e-mail: usamadgk@mul.paknet.com.pk.

In this paper, the thermomechanical processing treatments and intercritical heat treatments were designed to study their affect on the martensitic hardenability of austenite.

## 2. Experimental Work

### 2.1 Material

The composition of the steel (weight percent) employed in the present study is listed in the following table.

Type	C	Si	Mn	P	S	Cr	Mo	Ni	Cu
A	0.16	0.24	1.03	0.010	0.009	0.14	0.04	0.15	0.20
B	0.088	0.26	1.2	0.010	0.009	0.78	0.04	0.15	0.20

The material was supplied in the form of hot-rolled slabs, and plates. Metallographic investigation of the as-received microstructure showed that it consisted of unbanded ferrite and pearlite and traces of martensite or retained austenite in both steels. In order to study the effect of intercritical annealing temperature on the volume fraction of austenite, specimens approximately 10 mm square and 2 mm thick were heat treated in the range of 725 to 830 °C (with approximately 15 °C intervals) in an argon atmosphere for 20 min and then quenched in ice brine. The austenite volume fraction was measured by the point counting technique.

### 2.2 Specimen Preparation

For rolling experiments, a set of specimens (both for steels A and B) with initial thickness of 10 mm and area of 60 × 30 mm were machined, so that, after rolling to 50% reduction, all the specimens would exit from the rolls at a common thickness of 5 mm. In addition, another set of specimens with 5 mm initial thickness and 50 × 50 mm area were heat treated, but were not rolled. The purpose of the common thickness of 5

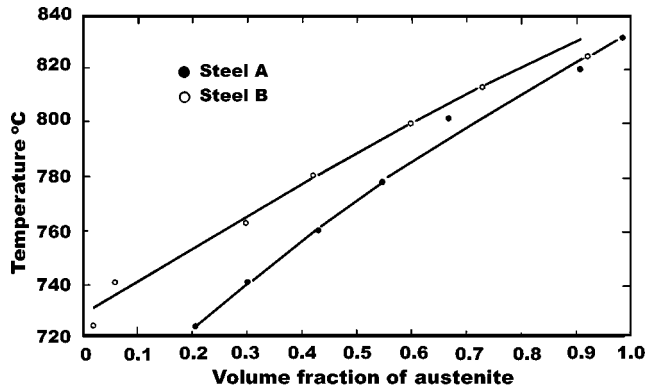


**Fig. 1** Dependence of austenite contents on intercritical annealing temperature of both steels A and B

mm for rolled and not rolled specimens was to ensure that the cooling rate would be the same in both.

### 2.3 Intercritical Heat Treatment at Selected Temperatures

For the purpose of studying the effect of warm rolling at the intercritical annealing temperature (ICAT) on the martensitic hardenability of austenite, the experiments were divided into two groups.

For group 1, the specimens of steels A and B with initial thickness of 5 mm and area of  $50 \times 50$  mm were heat treated for 20 min at 780 and 790 °C, respectively. These temperatures were selected to obtain a planned austenite volume fraction of 55% based on the results of the experiments described in Fig. 1. At the end of the heat treatment, the specimen was removed from the furnace and plunged into one of the following cooling media:

- a quench tank containing ice brine (10% NaCl, at  $-7$  °C),
- a quench tank containing cold water,
- a quench tank containing hot water,
- a quench tank containing boiling water,
- a quench tank of containing oil (fensu 68) at room temperature),
- hot air blast,
- still air, and
- a box containing vermiculite.

In group 2, the thermomechanical treatment was carried out in order to study the effect of controlled rolling on the martensitic hardenability of the austenite.

Specimens of steels A and B with initial thickness of 10 mm were intercritically annealed at 780 and 790 °C, respectively, in a muffle furnace situated close to and facing the entry to the rolls. After the required soaking time, the door of the furnace was opened and the specimen was pulled by its handling rod from the furnace and put directly into the rolls. Immediately after exit from the rolls, it was cooled in one of the media listed above.

The volume fractions of the constituents present after cooling were determined by quantitative optical metallography.

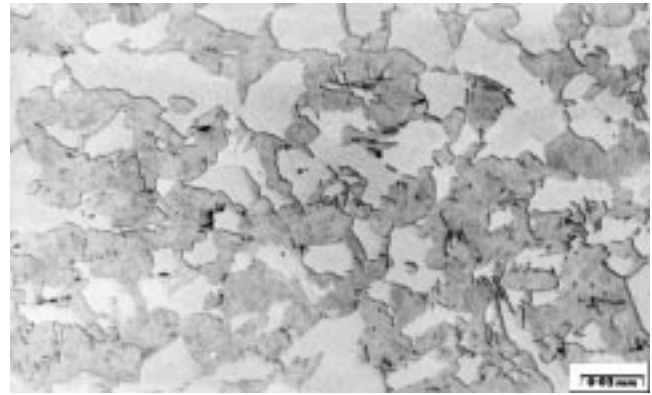


**Fig. 2** Microstructure of steel A heat treated at 780 °C followed by brine quench shows ferrite martensite phases

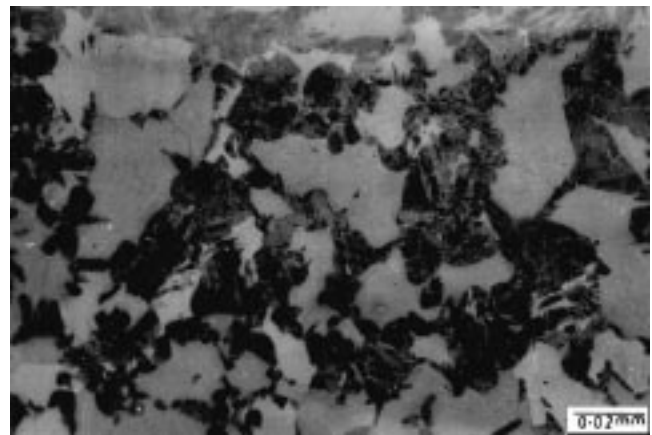


**Fig. 3** Microstructure of steel B heat treated at 790 °C followed by brine quench shows ferrite martensite phases

## 3. Results and Discussion

### 3.1 Effect of Intercritical Annealing Temperature on Volume Fraction of Austenite

Figure 1 shows the variation of austenite content with intercritical annealing temperature for both steels A and B. It can be seen that the volume fraction of austenite increased with the increase in the intercritical annealing temperature for both steels A and B. However, the volume fraction of austenite at any temperature for steel B was less than that for steel A because of the smaller amount of carbon content and higher content of Cr in steel B; Cr is a ferrite stabilizing agent that raises the  $A_{e3}$  temperature.

### 3.2 Microstructure Map Developed at Zero Reduction

The dual-phase structures developed after intercritical annealing of steels A and B at 780 and 790 °C, followed by brine quenching, are shown in Fig. 2 and 3, respectively. At slower cooling rates, new ferrite formed before the remaining

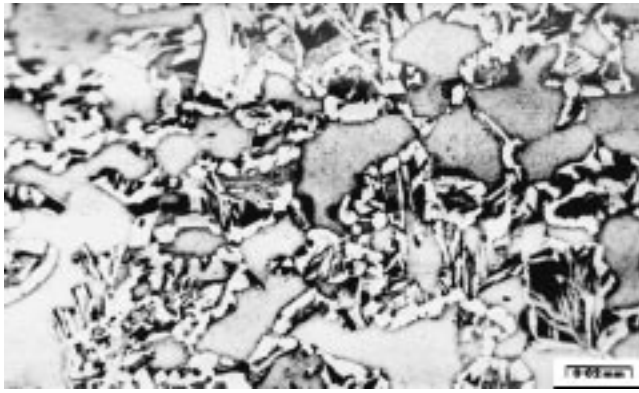


Fig. 4 Microstructure of steel A heat treated at 780 °C followed by quenching in boiling water shows the presence of epitaxial ferrite

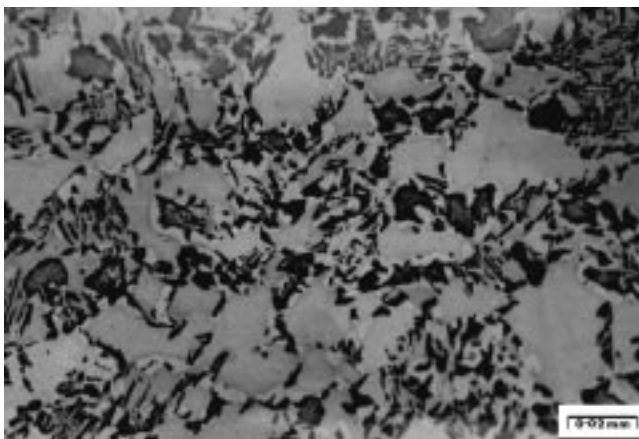


Fig. 5 Microstructure of steel B heat treated at 790 °C followed by quenching in boiling water shows the presence of epitaxial ferrite

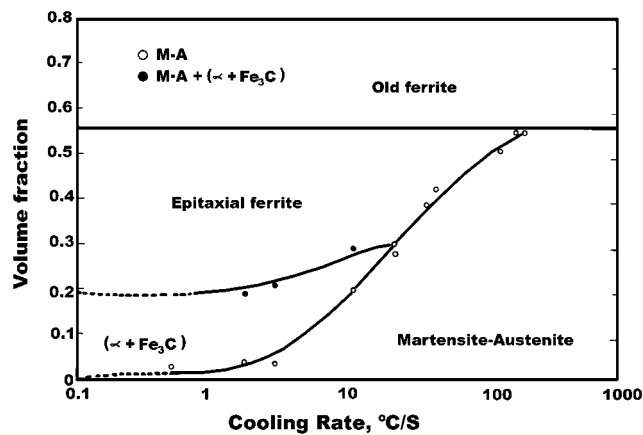


Fig. 6 Quantitative microstructure map showing the effect of cooling rates on the microstructure of steel A ICAT at 780 °C with 0% reduction

austenite transformed to martensite, as shown in Fig. 4 and 5. In Fig. 6 and 7, the cumulative volume fractions of microstructural constituents present after intercritical annealing at 780 and 790 °C are plotted versus cooling rate. Individual determinations of the austenite present at the intercritical temperature

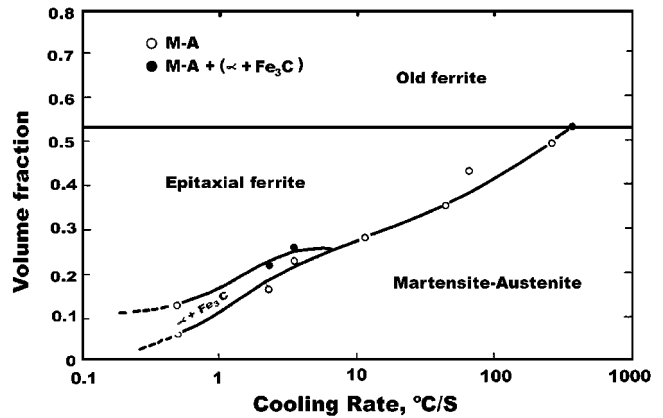


Fig. 7 Quantitative microstructure map showing the effect of cooling rates on the microstructure of steel B ICAT at 790 °C with 0% reduction

varied slightly around the mean value of 55.7 and 53% for steels A and B, respectively.

A normalizing factor was obtained for each individual austenite value,  $f\gamma$ , as the ratio of  $0.557/f\gamma$  and  $0.53/f\gamma$ , where 0.577 and 0.53 are the average values of all the volume fractions of austenite of steels A and B, respectively. Each value of the volume fraction of martensite and ferrite/carbide aggregate was normalized by multiplying by the respective normalizing factor, and all of the values are plotted in Fig. 6 and 7. The normalizing correction was smaller than 3%. The reason for doing this was to smooth out variations arising from random deviations in the volume fraction of austenite from which the various constituents were formed.

It can be seen from Fig. 6 that, even at the fastest cooling rate that was used, a small amount of epitaxial ferrite was formed before the onset of martensite transformation. The amount of epitaxial ferrite increased with decreasing cooling rate until approximately 23 °C/s was reached. At cooling rates less than this, ferrite/carbide was formed, the amount of which increased at the expense of martensite at still slower cooling rates. Within the range of cooling rates studied below 23 °C/s, the amount of epitaxial ferrite increased only slightly. Figure 7 shows that, at the highest cooling rate, no epitaxial ferrite was formed. The amount of epitaxial ferrite increased with decreasing cooling rate, at the expense of martensite. The ferrite carbide appeared at a critical cooling rate of 6.4 °C/s, and its amount increased with decreasing cooling rate.

The comparison of microstructure maps for steels A and B is shown in Fig. 8. It can be seen that in steel B the critical cooling rate for ferrite-carbide aggregate was 6 °C/s compared to 23 °C/s in steel A. However, steel A produced more martensite than steel B at cooling rates higher than 32 °C/s. These differences arise from the different carbon and alloy contents in the two steels, are important to dual-phase technology, and do appear to have been quantified in this way in literature previously. In normal heat treatment, in which steels are fully austenitized before quenching, a lower carbon content, as in steel B compared with steel A, reduces hardenability, shortening the time required for transformation to ferrite. In dual-phase steel, a lower carbon content of the steel reduces the carbon concentration present in the austenite volume if the ICAT is varied to provide the same volume fractions of austenite.

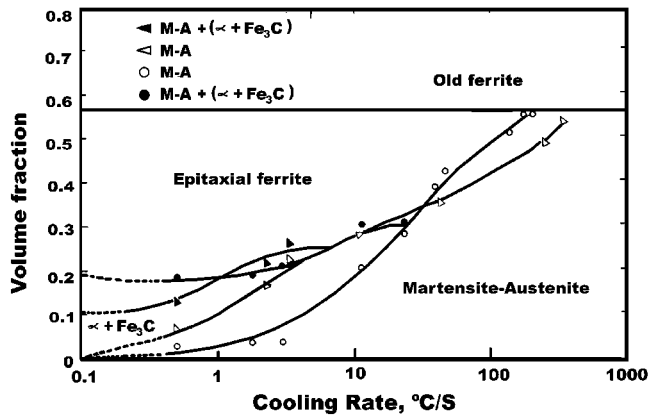


**Fig. 8** Quantitative microstructure map showing the effect of cooling rates on the microstructure of steels A and B ICAT at 780 and 790 °C, respectively, with 0% reduction

According to Priestner and Ajmal,<sup>[2]</sup> this increases the critical cooling rate at which a specified fraction of the austenite will transform the martensite, *i.e.*, will reduce hardenability. This does seem to be the effect of lower carbon content in steel B compared with steel A for cooling rates faster than about 32 °C/s. The effect of adding chromium in normal heat treatment, is to slow ferrite and pearlite formation and thus increase hardenability. In steel B, this effect of chromium clearly offsets the effect of lower carbon content only; at slower cooling rates, considerably more martensite is obtained in steel B than in steel A, despite the fact that critical cooling rates for full transformation of austenite are much higher in steel B than in steel A. Further, the effect of the lower carbon content of steel B causes lower cooling rates, where the quantity of pearlite or bainite formed is much less than in steel A.

The implications with respect to dual-phase steel technology can now be seen clearly. The benefit of adding chromium is not to reduce the quenching power needed to get full conversion of austenite to martensite, but rather to obtain useful quantities of martensite at low quenching power together with a reduction in the risk of obtaining damaging quantities of pearlite or bainite.

### 3.3 Microstructure Map after 48% Reduction

Figures 9 and 10 show the microstructure of steel A intercritically annealed at 780 °C and steel B intercritically annealed at 790 °C and warm rolled at those temperatures to 48% reduction before quenching into iced brine. At slower cooling rates (oil quenching for steel A and boiling water quenching for steel B), new ferrite formed before the remaining austenite transformed to martensite, as illustrated in Fig. 11 and 12. The microstructure maps of material rolled to 48% at 780 and 790 °C are presented in Fig. 13 and 14 for both steels. It was observed that, even at the highest cooling rate, approximately 10% of austenite transformed to ferrite due to a temperature drop of approximately 65°C during rolling. The data were normalized to the mean amount of austenite determined over all the specimens, as discussed in Section 3.2.

Figures 15 and 16 show a comparison of microstructure maps for 0 and 48% reductions of steels A and B, respectively.

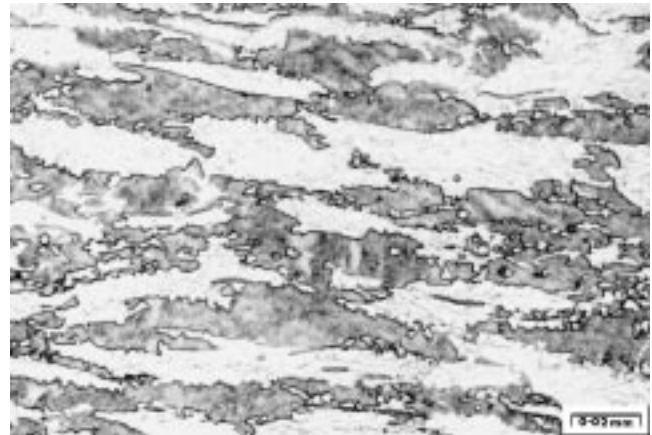


**Fig. 9** Microstructure of steel A warm rolled to 48% at 780 °C followed by brine quench shows fibrous martensite

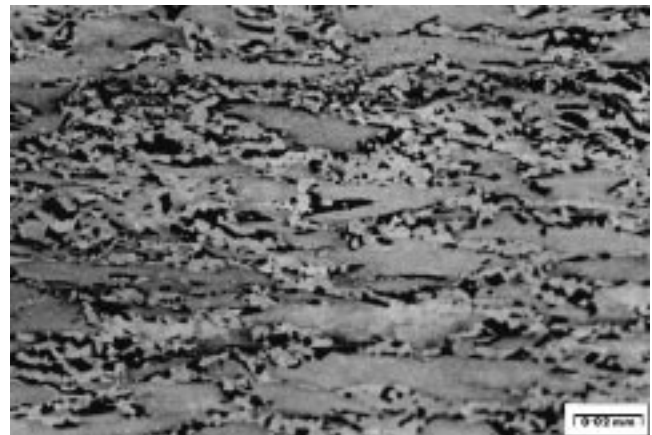


**Fig. 10** Microstructure of steel B warm rolled to 48% at 790 °C followed by brine quench shows fibrous martensite



**Fig. 11** Microstructure of steel A warm rolled to 48% at 780 °C followed by oil quench shows the presence of epitaxial ferrite

Several authors<sup>[3–6]</sup> have reported effects of prior hot deformation of fully austenitized steel on subsequent transformation to

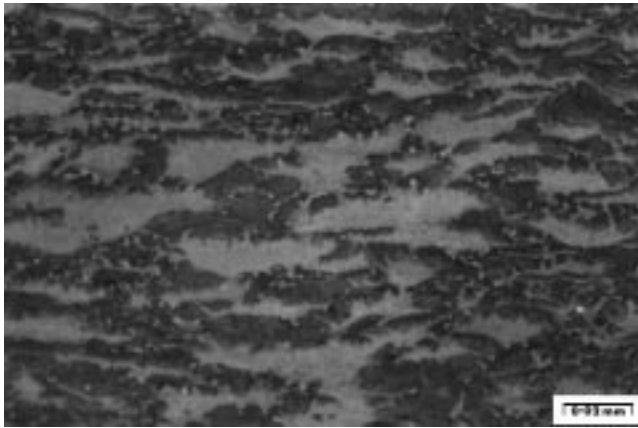


Fig. 12 Microstructure of steel B warm rolled to 48% at 790 °C followed by boiling water quench shows the presence of epitaxial ferrite

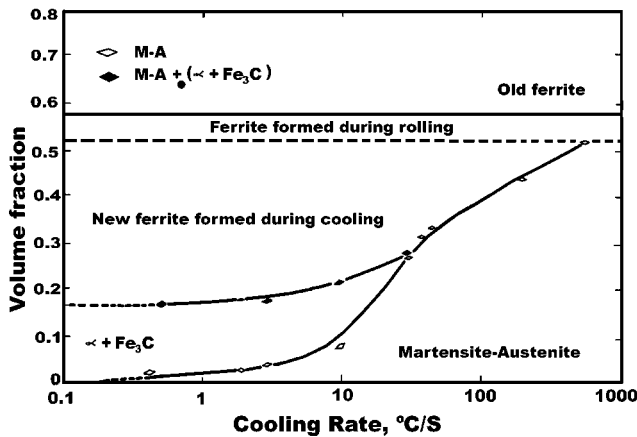


Fig. 13 Quantitative microstructure map showing the effect of cooling rates on microstructure of steel A ICHT at 780 °C with 48% reduction

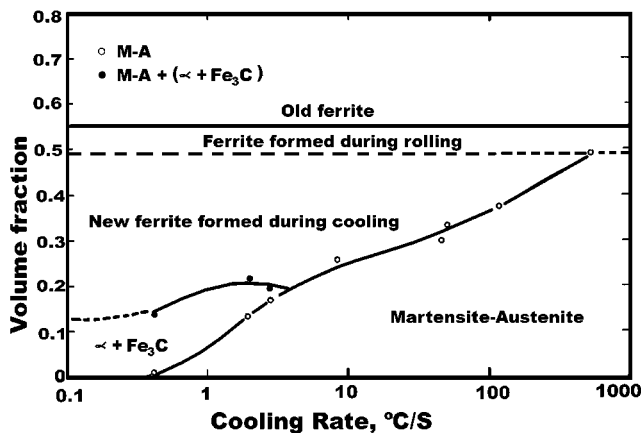


Fig. 14 Quantitative microstructure map showing the effect of cooling rates on microstructure of steel B ICHT at 790 °C with 48% reduction

ferrite. The deformation of austenite at a temperature where it does not recrystallize produces sets of roughly parallel bands,

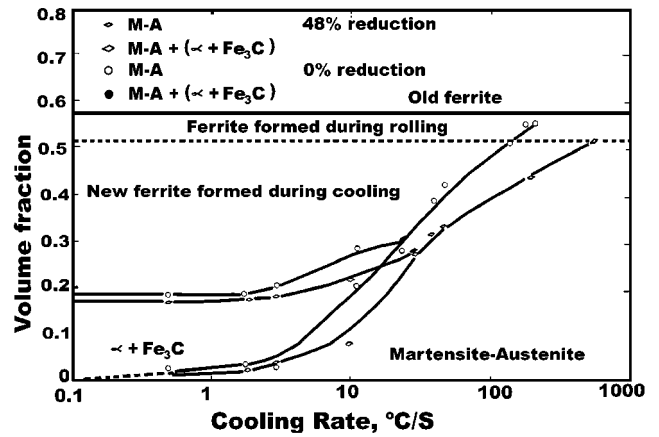


Fig. 15 Microstructure map showing the effect of cooling rates on the microstructure of steel A with 0 and 48% reduction

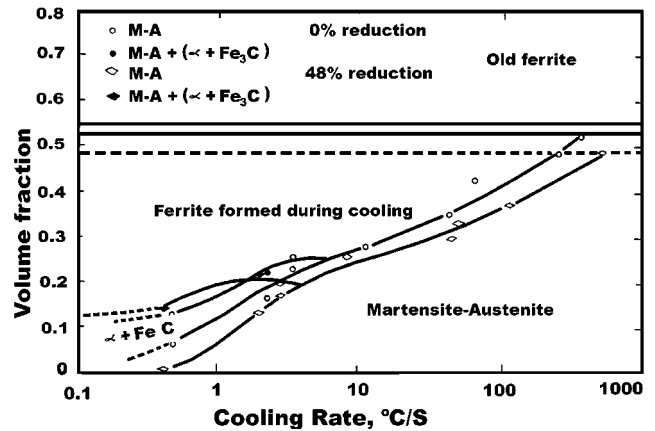


Fig. 16 Microstructure map showing the effect of cooling rates on the microstructure of steel B with 0 and 48% reduction

called deformation bands, within the grains. During quenching and after deformation,  $\alpha$  grains are nucleated at these deformation bands as well as at  $\gamma$  grain boundaries. Effectively, the total grain boundary area is increased due to the increasing aspect ratio of austenite grains with deformation, as well as by the presence of deformation bands. This stimulus to the formation of ferrite thus reduces the martensitic hardenability of the austenite.

The situation becomes more complex when the deformation is applied in the intercritical phase field, because nucleation is not involved when ferrite grows epitaxially from the existing ferrite. However, the increased  $\alpha/\gamma$  interfacial area that results from rolling should be expected to increase the amount of epitaxial ferrite grown during the given quench, at the expense of martensite. The present results confirm this suggestion, as shown in Fig. 15 and 16.

The observation that rolling at the intercritical temperature reduced the amount of martensite formed on cooling over the entire range of cooling rates contradicts previous work by Ajmal and Priestner.<sup>[7]</sup>

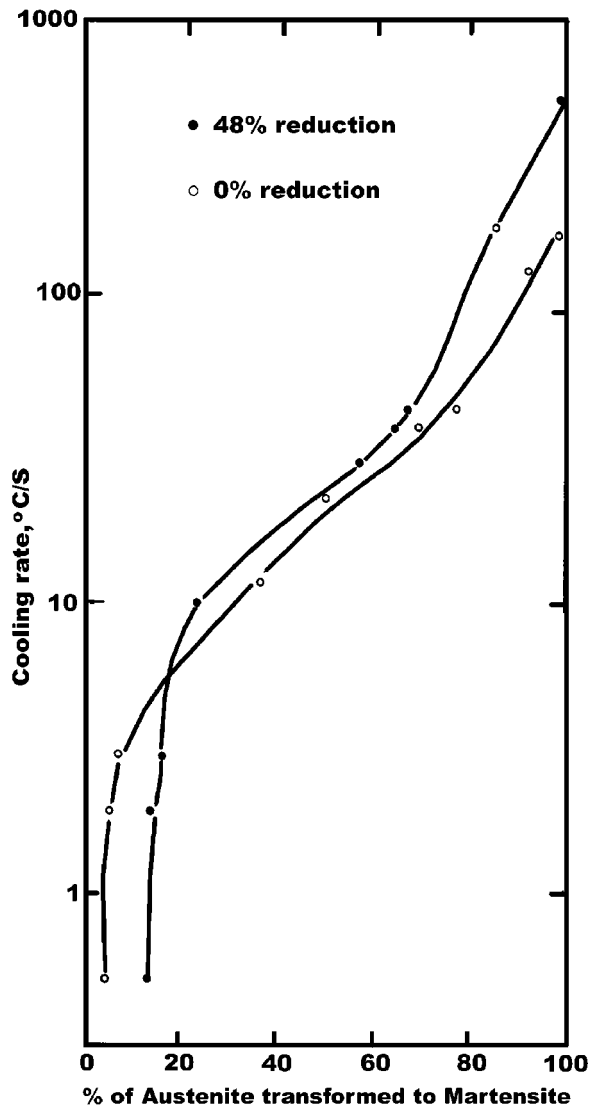


Fig. 17 Fraction of austenite transformed to martensite as a function of cooling rate, steel A

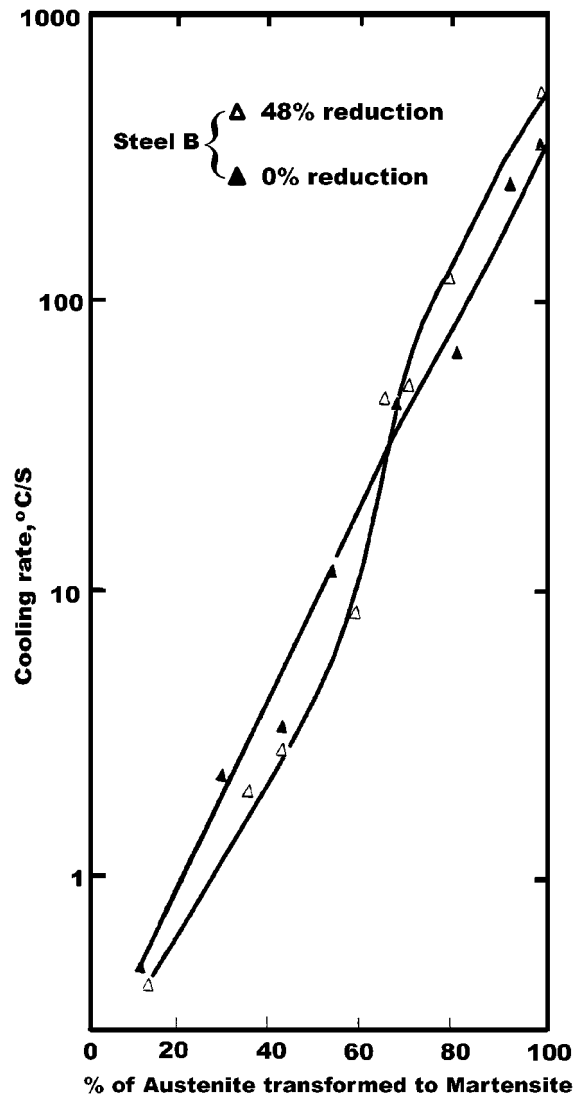


Fig. 18 Fraction of austenite transformed to martensite as a function of cooling rate, steel B

### 3.4 Hardenability of Austenite

In the traditional hardening heat treatment, when steels are quenched from the fully austenitic region of the phase diagram, the most important microstructural variables that influence the hardenability are the composition of the austenite and its grain size. The hardenability increases with increasing austenite grain size, due to the decrease in grain boundary area and the consequent reduction in the density of sites and in the rate of nucleation of ferrite and pearlite, and the ferrite and pearlite reactions are slowed down. Most alloying elements play an important role in slowing the ferrite and pearlite reactions, and thus also increase the hardenability of the steel. In the case of dual-phase steel, the nucleation of new ferrite is not essential since the ferrite existing at ICAT can grow epitaxially into austenite. Also, the volume of austenite formed during intercritical annealing is dependent upon the intercritical temperature.<sup>[8,9]</sup> Thus, the hardenability of the austenite may be assessed more fundamentally in terms of the fraction of austenite, which transforms to

martensite, rather than as the fraction of the total volume of steel, which transforms to martensite. Also, austenite present at the intercritical temperature contains few grain boundaries. The rate of ferrite formation is not controlled by its nucleation rate, but by the rate of growth of existing ferrite.

The microstructure maps in Fig. 6 and 13 and 7 and 14 are summarized in the form of an austenite → martensite hardenability diagram in Fig. 17 and 18. Approximately 10% of austenite present transformed to ferrite during rolling. In Fig. 13 and 14, the fraction of the austenite still present after rolling and just before quenching, and which transformed to martensite, is plotted. It can be seen that, at a higher cooling rate than 6 °C/s for steel A and 20 °C/s for steel B, the volume fraction of austenite that transformed to martensite in the rolled material was less than in the nonrolled material. Data were obtained in a similar way by Priestner and Ajmal<sup>[2]</sup> for a steel containing 0.11% C and 1.5% Mn. It is clear that in the present work rolling at the intercritical annealing temperature decreased the

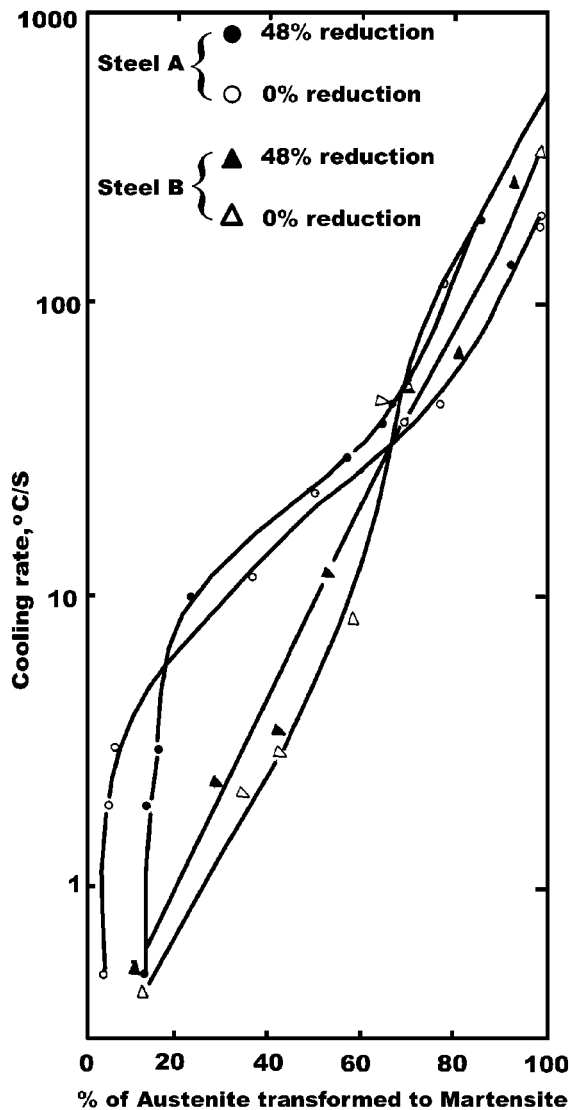


Fig. 19 Fraction of austenite transformed to martensite as a function of cooling rate, steels A and B

hardenability of the austenite remaining after rolling, whereas, in Priestner and Ajmal's work, rolling increased the hardenability of the austenite.

The apparent effect of rolling on the austenite  $\rightarrow$  martensite hardenability is complicated by the fact that the increase in ferrite by about 10% during rolling is accompanied by an increase in the carbon content of the remaining austenite. This would be expected to increase the hardenability of that austenite relative to the hardenability of the austenite present before rolling, apart from any direct effect of the rolling. The direct effect of rolling, therefore, must have been larger than that shown in Fig. 17 and 18. Direct comparison (Fig. 19) of both steels A and B showed that, in both, rolling decreased the hardenability at fast cooling rates and increased it at low cooling rates. The crossover point was at a very much lower cooling rate for steel A. The austenite in steel A was much less hardenable than that of steel B at the lower cooling rates.

At a constant volume fraction of austenite particles, the

interfacial area increases rapidly with the decrease in particle size. Priestner<sup>[10]</sup> suggested that, since epitaxial ferrite forms by regrowth of existing ferrite into the austenite, the volume that forms is the product of interfacial area, average growth rate during cooling, and time taken to cool to the  $M_S$  temperature. He found that the fraction of the austenite that remained at the  $M_S$  temperature and which then transformed to martensite depended very strongly on the fineness of the dispersion of austenite particles. In his model, he also suggested that warm rolling in the  $(\alpha + \gamma)$  phase field elongated austenite particles in the rolling direction, thus increasing their interfacial area without changing their volume. Warm rolling, therefore, should decrease the martensitic hardenability of the austenite. The present work is in agreement with Priestner's model.

As mentioned before, rolling in the two-phase region of the phase diagram would be expected to increase the interfacial area. This, in turn, should promote the formation of ferrite during cooling and thus decrease the martensitic hardenability of the austenite. The results presented here suggest that this is true for cooling rates faster than 6 and 20 °C/s for steels A and B, respectively.

#### 4. Conclusions

Low-carbon, low-alloy steels were intercritically heat treated and thermomechanically processed to study the martensitic hardenability of austenite present.

In thermomechanically processed materials, approximately 10% of the austenite present at the intercritical annealing temperature transformed to ferrite during rolling, due to a temperature drop of approximately 65 °C during rolling. The present results strongly suggest that rolling decreased the hardenability of the remaining austenite. For example, Fig. 19 (steel A) shows that, at all cooling rates higher than 6 °C/s, the volume fraction of austenite that transformed to martensite in rolled material was less than in the nonrolled material. Similarly, for steel B, at all cooling rates higher than 20 °C/s, the volume fraction of austenite that transformed to martensite in rolled material was less than in the nonrolled material.

This agrees with the view that the rolling in the two-phase  $(\alpha + \gamma)$  field increased  $\alpha/\gamma$  interfacial area, thus promoting the formation of ferrite during cooling and decreasing the martensite hardenability of austenite.

#### References

1. R.D. Lawos, D.K. Matlock, and G. Krauss: in *Fundamentals of Dual-Steel*, R.A. Kott and B.L. Bramfitt, ed., AIME, New York, NY, 1981, p. 347.
2. R. Priestner and M. Ajmal: *Mater. Sci. Technol.*, 1987, vol. 3, pp. 360-64.
3. Y.E. Smith and C.A. Slebert: *Metall. Trans.*, 1971, vol. 2, pp. 1171-25.
4. J.J. Jonas and R.A. do Nascimento: in *Fundamentals of Dual-Phase Steels*, R.A. Kot and J.W. Morris, eds., AIME, New York, NY, 1981, pp. 95-112.
5. H. Takeehi, W. Matsuda, H. Tamehiro, M. Ohashi, and H. Nakasug: in *Micron 82*, ASTM, 1982, pp. 149-71.
6. T. Kota, K. Hashinguchi, I. Takahashj, T. Irie, and N. Ohashi: in *Fundamentals of Dual-Phase Steels*, R.A. Kot and B.L. Bramfitt, eds., AIME, New York, NY, 1981, pp. 199-220.
7. M. Ajmal and R. Priestner: *Thermec 88*, Int. Conf. on Physical Metal-

- lurgy of TMP of Steel and Other Metals, Tamuta, ISIJ, 1988, pp. 624-91.
8. E. Ahmad and R. Priestner: *Proc. 5th Int. Symp. on Advanced Materials*, 1997, pp. 365-69.
  9. M. Sarwar and R. Priestner: *J. Mater. Eng. Performance*, 1999, vol. 8 (3), pp. 380-84.
  10. R. Priestner: *Phase Transformation*, 87, Institute of Metals Conf., Cambridge, July 6–10, 1987.